JOURNAL GEOLOGICAL SOCIETY OF INDIA
Vol.91, January 2018, pp.15-24

Seismic Moment Release Data in Earthquake Catalogue: Application of Hurst Statistics in Delineating Temporal Clustering and Seismic Vulnerability

Basab Mukhopadhyay* and Diptansu Sengupta

Geological Survey of India, Central Headquarters, 29 J. L. Nehru Road, Kolkata - 700 016, India
***E-mail:** basabmukhopadhyay@gmail.com

ABSTRACT

Sequential cumulative moment release data of macro-earthquakes (Mw≥4.3) of seventeen seismic zones (A to Q) belonging to NE-Himalaya, Burmese-Andaman arc and West-Sunda arc are analysed by Hurst analysis, a non-parametric statistical procedure to identify clustering of low and high values in a time series. The moment release in a zone occurs in alternate positive, negative and positive sloping segments forming a wave like pattern with intervening small horizontal segment. The negative sloping segments indicate decelerated moment release pattern or temporal slackening of elastic strain release with high b–value (>0.95). The horizontal segment indicates temporal clustering of moderate magnitude events/seismic moments with moderate b-values (0.8–0.95). The positive segment is characterised by accelerated moment release within a short span of time indicating temporal clustering of larger magnitude earthquakes/ seismic moments and exhibit lowest b–value (<0.7). All zones attest moderate to high Hurst K values, range 0.7-0.86. The pattern in Hurst plots, specially a reversal of trend after prolong negative slope is used for earthquake prognostication in the seismic zones. Our analysis shows that most of the zones register a notable reversal of Hurst clustering trend after a prolonged negative slope which is accompanied by a major earthquake near its end. However, South Burma region (Zone-I) and Tripura fold belt and Bangladesh Plain (Zone-K) do not show any moderate or large shock around the end of the negative sloping trend in Hurst plot. Hence, these two zones can be considered more prone to produce moderate to larger earthquakes in future.

INTRODUCTION

Earthquake events of similar magnitude occurring close together in space produce spatial seismic clusters. A temporal seismic cluster is suspected in a region if it consists of successive multiple earthquakes of magnitudes either greater or less than a threshold value originating within an acceptable time period. In seismology, foreshock – mainshock – aftershock sequences form spatial clusters which can be recognised in an earthquake catalogue and seismicity map with little effort. But, moderate to large magnitude earthquakes and its corresponding moment release data also occur as temporal clusters which cannot be easily delineated by visual search within a catalogue or seismic map. The degree of such clustering is usually reflected by alternate temporal clustering of high, moderate and low seismic moment values in an earthquake catalogue where successive moment release values form a natural time series. The tendency of this type of temporal clustering within a catalogue is best identified through a non-parametric statistical procedure commonly known as Hurst statistics and corresponding Hurst plot, developed by Hurst (1951, 1956). This rescaled range analysis of Hurst (Feder, 1988) has been applied on many sequential time series data that occur in nature to quantify and classify high and low clustering hidden in dataset of various geo-scientific discipline (Wallis and Matalas, 1970, 1971; Haslett and Raftery, 1989; Evans, 1996; Chen and Hiscott, 1999; Weber and Talkner, 2001; Mukhopadhyay et al., 2003; Koutsoyiannis, 2003; Hernandez-Martinez et al., 2013; Feng and Zhou, 2013; Markonis and Koutsoyiannis, 2013;Shi et al., 2015; Miao et al., 2015), including yearly cumulative earthquake moment release data for pattern recognition in tectonic zones of Himalayas with an aim to identify precursor(s) for impending events (Mukhopadhyay et al., 2009).

In the present paper, the sequential moment release data of macro-earthquakes (Mw ≥ 4.3) from January 1965 to June 2016 within the bounding latitude 0°–32° N and longitude 87°–98° E comprising of tectonic/seismic domains: NE Himalaya including Tibet (NEHT), Burmese–Andaman Arc System (BAAS) and West Sunda Arc (WSA) have been analysed subdividing the area into seventeen seismic zones (A to Q) solely depending on seismo-tectonic criteria. The temporal clustering within the sequential moment release data of earthquakes in those zones (A to Q) are quantified through Hurst statistics. The statistics compute degree of clustering in moment release value by a scalar coefficient Hurst K. The seismic characteristics of the zone are illustrated by corresponding b-value from earthquake magnitude data. Further, within a zone, the alternate clustering of high, moderate and low moment release values in the dataset is identified by the Hurst plot. Calculated b-values of the earthquakes showing high, moderate and low moment release trends in a Hurst plot are further used to define the dynamic nature of the seismic crust during successive time period within a zone. The aim of the present paper is to synthesize all available trends in Hurst plots and finally use it as a tool to identify temporal seismic clustering of moment release data within earthquake catalogue in the study area and to identify zones which may be seismically vulnerable.

EARTHQUAKE CATALOGUE

The earthquake catalogue for the period from January 1965 to June 2016 is extracted from ISC database for latitudes 0° - 32° N and longitudes 87° E- 98° E. The earthquake magnitudes (M_S, $m_b$etc) of the catalogue has been converted to a uniform scale, moment magnitude (M_w) following the conversion formula given by Scordilis (2006). For magnitude completeness, the methodology based on the assumption of self-similarity (Wiemer and Wyss, 2000) has been applied on the earthquake catalogue to estimate the magnitude of completeness (Mc). The *b*-value is estimated from Frequency-magnitude distribution of the earthquake data for different periods in different areas using the MAXC approach (Wiemer and Wyss, 2000) with magnitude completeness (Mc≥4.3). Further, the seismic-moment M_0 (in dyne cm) for individual earthquake event ($M_w \geq 4.3$) is calculated using the equation, log M_0 =C*M_w + D (eq. 1) where

0016-7622/2018-91-1-15/$ 1.00 © GEOL. SOC. INDIA | DOI: 10.1007/s12594-018-0815-z

C = 1.5 and D = 16.05 (Hanks and Kanamori,1979; McGuire, 2004). Hence, the catalogue contains both magnitude and corresponding moment release data for sequential earthquakes.The *b*-value is calculated by the maximum likelihood method (Aki, 1965) with the equation $b = (\log_{10} e) / (M_{av} - M_{min})$ (eq. 2), where M_{av} is the mean magnitude above the threshold M_{min}. The maximum-likelihood method provides the least biased estimate of *b*-value (Aki, 1965). The confidence limit of the *b*-value is inversely proportional to the square root of the number of events, thus error in *b*-value is estimated by the formula $b/\sqrt{N}$, where N is the number of earthquakes used for *b*-value calculation (Aki, 1965).

HURST STATISTICS AND PLOT

Hurst (1951, 1956) proposed a non-parametric statistical application popularly termed as Hurst statistics while working on long-term storage of reservoirs along river Nile in Egypt. He deduced a relationship that states $R/S \sim N^h$ where R is the maximum range of cumulative departure from mean annual discharge of river, N is the year of observations, S is the standard deviation of river discharge and 'h' is the coefficient. Hurst approximated the coefficient 'h' by another scalar K where K is equal to $\log(R/S)/\log_{10}(N/2)$. It is found that natural sequences with large number of observations follow Hurst phenomenon and yield a K value greater than 0.5 (Wallis and Matalas, 1971). A Hurst exponent (K) close to 0.5 is thus indicative of a Brownian time series where there is no correlation between the present observations and an estimated result for future (Mandelbrot and Hudson, 2004). A Hurst exponent value between 0 and 0.5 is indicative of anti-persistent behaviour i.e. the tendency for the time series to revert to its long-term mean value. Whereas, a Hurst exponent (K) between 0.5 and 1.0 indicates persistent behaviour i.e. an increase in values will most likely to be followed by an increase in the short term, and a decrease in values will most likely to be followed by another decrease in the short term (Mansukhani, 2012) and hence indicating distinct temporal clustering in datasets. Further, Hurst (1951, 1956) observed that a natural process (with large number of observations) occurring in irregular groups of high and low values show high K values greater than 0.5. Alternately, where the number of observations (n) is small, an estimator H is calculated by dividing the log-transformed ($\log_{10}$) observations into n number of subseries (Wallis and Matalas, 1971). For each sub-series the value of Rn/Sn is calculated. The slope of regression line in log(Rn/Sn)/log(n) plot gives the value of H. For large values of N, Chen and Hiscott (1999) and Mukhopadhyay et al.(2003) observed that K value lies between 0.5 and 0.9.

The seismic moment values calculated by equation 1 of successive earthquake events for an individual zone are taken as a time series. To calculate K for N number of observations, the seismic moment values are transformed logarithmically (base $\log_{10}$). Mean (M) and standard deviation (S) of the log transformed moment data are calculated. From each moment data, the mean is subtracted and then cumulative difference from the mean is computed by adding the values in the series. This cumulative departure from mean is plotted against sequential number of the event / year to generate the Hurst plot. Range (R) is calculated as the difference between the maximum and the minimum value of the cumulative deviation in the Hurst plot, and K is calculated by the formula $\log (R/S) / \log_{10}(N/2)$, where N is the total number of observations. The moment release pattern can be graphically illustrated in Hurst plot where cumulative difference from the mean moment is plotted against sequential observation / year. The plot contains three distinct trends; positive, horizontal and negative sloping segments. The significance of which is illustrated later on.

DELINEATION OF SEISMIC ZONES

The study area consisting of 2800 km long tectonic domain covering NE Himalaya including Tibet (NEHT), Burmese–Andaman Arc System (BAAS) and West Sunda Arc (WSA) together constitute a prominent subducting plate margin in the NE Indian Ocean and corresponding land part in India and Burma. The zone serves as the tectonic link between the Western Pacific Arc System in the South-east with the Himalayas in the north. The northernmost segment of the NE Himalayan arc, a typical collisional front where north bound India and south bound Eurasia collision ends at Eastern Himalaya syntax around Namcha Barwa. Further south, BAAS in Burma where a subduction zone is clearly discernible in a land environment delimited by Eastern Boundary Thrust (EBT) with a frontal folded belt of Tripura and Bangladesh, and a stable Shan plateau in the back. Further south, the oblique ocean-ocean subduction of Indian plate under SE Asian plate is manifested by tectonic elements related to convergent tectonic margin in Andaman-Sunda Arc. The elements are a trench (Andaman trench), a sedimentary outer arc system (from Andaman to Nias island), volcanic arc (from Sumatra to Burma with dormant Narcondam and active Barren volcano in between) and a backarc spreading centre (Andaman Spreading Ridge - ASR). The entire area has experienced severe seismicity in the recent past with incidence of many moderate to large earthquakes like the great 2004 Sumatra earthquake (26.12.2004, M_w9.0), Nias earthquake (28.03.2005, M_w 8.6) along the plate interface and prominent intraplate strike-slip seismicity within Indo-Australian plate (10.01.2012, M_w7.2; 11.04.2012, M_w8.6 and 11.04.2012, M_w8.2).

The earthquake data with magnitude (Mw) greater than or equal to 4.3 are plotted in map (Fig.1) with suitable magnitude bins, superimposed on the tectonic elements compiled after Curray (2005). Within this varied tectonic scenario, entire study area is subdivided into seventeen seismic zones, A to Q (Fig.2). The geographical boundary of the zones are delineated taking into consideration various factors like variation in tectonic style; zones for thrust, strike-slip or normal earthquakes; ability to spawn large earthquake (Mw > 6) depending on present and past seismic records; presence of seismogenic transverse tear faults and other active seismogenic faults; spatial clustering zones of moderate to large earthquakes; speed of shear waves in different sectors wherever available, contrasting stress fields operate in top lithosphere in different zones, differential crustal structure as deduced from tomographic studies and its bearing to regional / local tectonics etc. The salient seismo-tectonic characters of the zones and seismic parameters calculated in the present study are tabulated (Table 1).

RELATIONSHIP BETWEEN TEMPORAL CLUSTERING AND *b*-VALUE

Hurst plots (Fig 3a-i) corresponding to the seventeen seismic source zones (A to Q in Figure 2) have been computed and analysed for temporal clustering pattern. From these plots (Figs 3a – 3i) for all the zones, it can be concluded that the moment release in a zone occurs in alternate positive, negative and positive sloping segments forming a wave pattern (Figs 3a to 3i), occasionally horizontal segment occurs within the negative sloping segment (Figs 3b and 3f). The Hurst plot pattern associated with the b-value calculations reveals few specific seismotectonic characteristics for each zone.

The lack of occurrence of major earthquakes in negative sloping segments indicate decelerated moment release pattern or temporal slackening of elastic strain release compared to the average (mean) moment release rate. This also indicates a temporal clustering of small magnitude earthquakes / seismic moments that exhibit high b–value (> 0.95) (Table 2). The high b-value indicates a large proportion of smaller earthquake events compared to large events with a possible low seismic hazard and thus probably corroborates with formation of numerous small cracks within the seismic volume.

The horizontal segment indicates temporal clustering of moderate

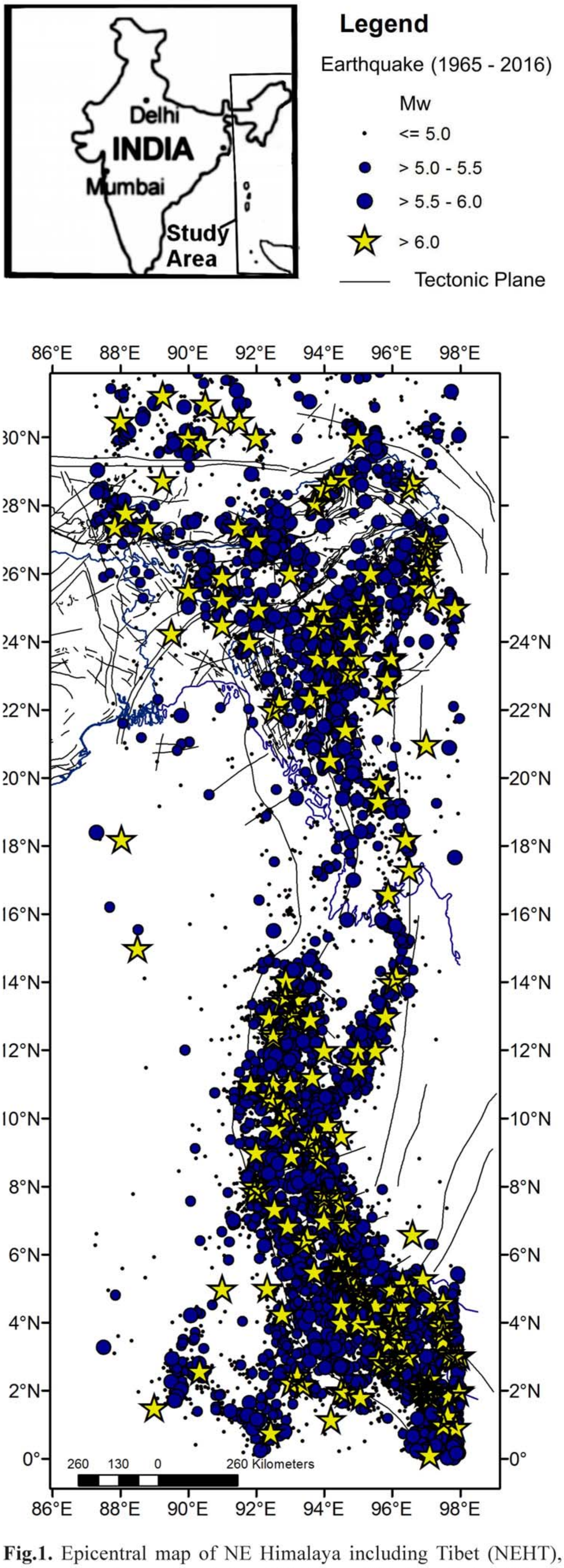

Fig.1. Epicentral map of NE Himalaya including Tibet (NEHT), Burmese–Andaman Arc System (BAAS) and West Sunda Arc (WSA) with earthquake data for the period 1965–2016 in different magnitude bins. Inset shows the study area.

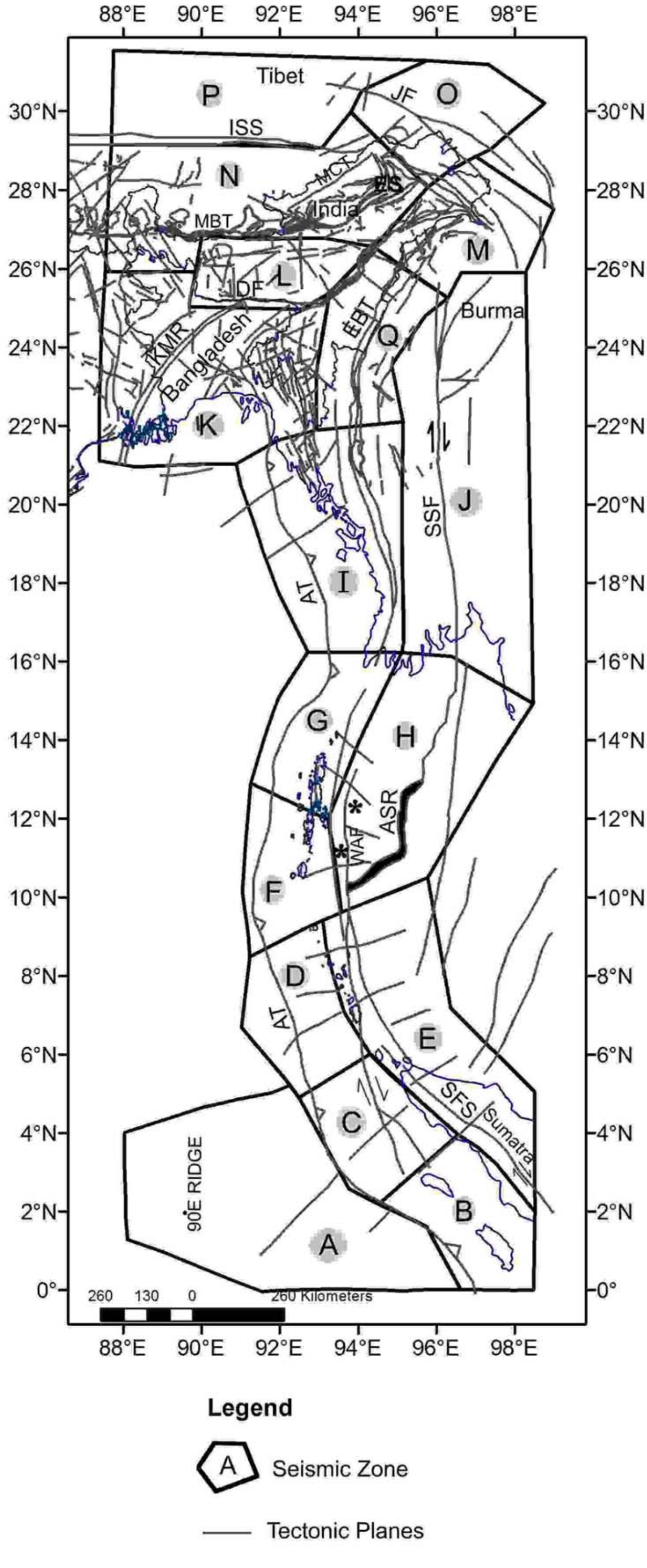

Fig.2. Spatial distribution of seventeen seismic zones (A to Q) delineated on the basis of variation of tectonic motif along the arc, seismogenesis, crustal heterogeneity and other geophysical parameters (see text) for Hurst analysis. AT – Andaman Trench, ASR- Andaman Spreading Ridge, EBT – Eastern Boundary Thrust, ISS – Indus Psangpo Suture, KMR – Kolkata Maimonsingh Ridge, SSF – Shan Sagaing Fault, SFS – Sumatra Fault System, WAF – West Andaman Fault.

Table 1. Characteristics of the Seismic Zones, A to Q of Fig.2.

Seismic Zone	Zone Name	Number of Earthquakes (N) ≥ Mc (4.3)	Dominant tectonics	Data Years [T]	Mmax Observed (year)	b-value ± error (maximum likelihood)	a-value =l log(ΣN/T)+ b*Mc
A	Indo-Australian Intra-plate Zone	905	Strike slip (oblique slip)	1966-2016 [51 years]	7.2 (2012)	0.95 ± 0.03	5.33
B	Nias Earthquake Zone	3616	Thrust	1965-2016 [52 years]	8.6 (2005)	0.88± 0.01	5.63
C	Sumatra Earthquake Zone	1783	Thrust	1967-2016 [50 years]	9.0 (2004)	0.78± 0.02	4.91
D	Nicober Island Zone	935	Thrust [48 years]	1969-2016 (2010)	7.0	0.9 ± 0.03	4.99
E	Sumatra Island Zone	2768	Strike slip (oblique slip)	1965-2016 [52 years]	6.6 (2015)	0.83± 0.02	5.30
F	South Andaman Zone	818	Thrust	1966-2016 [51 years]	6.5 (2008)	0.97± 0.03	5.38
G	North Andaman Zone	837	Thrust	1965-2016 [52 years]	6.7 (2009)	0.99 ± 0.03	5.46
H	Andaman Spreading Zone	1067	Strike slip and normal	1965-2016 [52 years]	6.1 (2010)	0.81± 0.02	4.80
I	South Burma Zone	335	Strike slip and thrust	1965-2016 [52 years]	6.2 (1994)	0.91± 0.05	4.72
J	Sagaing Fault Zone	457	Strike slip	1966-2016 [51 years]	6.2 (1991, 2012)	0.84± 0.04	4.57
K	Tripura Fold Belt and Bangladesh Plain	175	Thrust	1966-2016 [51 years]	6.0 (1988, 1997)	0.91± 0.07	4.45
L	Shillong Plateau	220	Strike slip (oblique slip)	1965-2016 [52 years]	5.6 (1971,1991, 2013)	0.93± 0.06	4.64
M	North Burma Fold-Thrust Belt	270	Strike slip (oblique slip) and thrust	1965-2016 [52 years]	6.4 (1970)	0.85± 0.05	4.37
N	NE Himalaya	326	Thrust	1965-2016 [52 years]	6.6 (2011)	0.82± 0.05	4.32
O	Eastern syntaxis – Jaili Fault Zone	329	Strike slip (oblique slip)	1965-2016 [52 years]	6.0 (2005)	0.75± 0.04	4.03
P	Tibetan Zone	338	Normal	1966-2016 [51 years]	6.1 (2008)	1.06± 0.06	5.38
Q	Central Burma Fold Thrust Belt	1066	Strike slip (oblique slip) and Thrust	1965-2016 [52 years]	6.9 (2016)	0.91± 0.03	5.23

magnitude events / seismic moments with moderate b-values (0.8 – 0.95) (Table 2). The earthquake magnitudes are of near average magnitude value of the entire catalogue. Moderate b-value indicates consolidation and stabilisation of the small cracks that have been generated earlier.

In contrary, the positive segment is characterised by accelerated moment release within a short span of time with temporal clustering of larger magnitude earthquakes / seismic moments and exhibit lowest b–value (<0.7). Low b – value is indicative of large proportion of bigger seismic events in comparison to smaller one which naturally indicates high seismic hazard. During this time, small cracks generated earlier are collapsed and joined with each other to generate large cracks and promote possible failure by formation of rupture within the seismic volume to generate large events.

PATTERNS ANALYSIS IN THE HURST PLOTS

Detail study of the alternate positive, horizontal and negative sloping moment release segments of the above mentioned Hurst plots in relationship with the occurrence of major shocks, gives an approximate idea about the elastic strain release periods for each seismotectonic zones as well as their interrelationship, and focus on seismic vulnerability. Although Hurst plots for the initial couple of decades may be misleading due to comparatively low level of detection of lower magnitude earthquakes, still the patterns may conclusively reflects few specific characteristics throughout the study area.

The Hurst plot patterns of zone B to G (Figs 3a – d), mostly representing the lower plate of Burmese-Andaman Arc System (BAAS) and West Sunda Arc (WSA), show a definite prolonged period of negative slope with very short termed horizontal segments of moment release acceleration in between. For zone B, a decelerating (negative) moment release segments (between 28.03.2005 and 30.07.2005, 1130 earthquakes) is followed by a horizontal moment release segment (between 30.07.2005 and 27.02.2008, 840 earthquakes) and another negative segment (between 27.02.2008and19.11.2013, 734 earthquakes). For zone C, a prominent occurrence of prolong negative segment (08.01.2005 and 09.12.2012, 936 earthquakes) takes place. For zone D, a decelerating (negative) moment release segments takes place between 06.01.2005 and 09.04.2013 with 503 earthquakes. In

Table 2. Characteristics of the temporal clusters as inferred from Hurst plots (Figs. 3a to 3i) of seismic zones (A to Q) of Fig.2.

Zone	Segments (see Figs 3a-i)	Nature of the segment	Nature of clustering (L, M, S)*	Time Period	No. of earthquakes in the segment	Major shock in in the segment (Mw)	b-value of the segment with error	Hurst K coefficient of the zone	b-value of the Zone with error
A	1	Horizontal	M	09.02.1966-14.03.2012	158	21.10.1969 (6.5) 10.1.2012 (6.6)	0.85±0.07		
	2	Positive slope	L	14.03.2012-12.04.2012	112	11.04.2012 (7.2), 11.04.2012 (6.6)	0.64±0.06	0.791	0.95±0.03
	3	Negative slope	S	12.04.2012-30.07.2013	532	-	1.17±0.05		
	4	Positive slope	L	30.07.2013-12.05.2016	103	-	0.79±0.08		
B	1	Positive slope	L	19.07.1965-28.03.2005	700	27.02.1974 (6.1), 02.11.2002 (6.3), 28.03.2005 (8.6)	0.71±0.03	0.754	0.88±0.01
	2	Negative slope	S	28.03.2005-30.07.2005	1130	28.03.2005 (6.1), 30.03.2005 (6.0), 16.04.2005 (6.0), 19.05.2005 (6.1)	0.96±0.03		
	3	Horizontal	M	30.07.2005-27.02.2008	840	-	0.87±0.03		
	4	Negative slope	S	27.02.2008-19.11.2013	734	06.04.2010 (6.7)	1.04±0.04		
	5	Positive slope	L	19.11.2013-14.06.2016	212	-	0.78±0.05		
C	1	Positive slope	L	25.02.1967-13.04.1995	220	-	0.64±0.04	0.7015	0.78±0.02
	2	Negative slope	S	13.04.1995-26.12.2004	181	26.12.2004 (9.0)	1.08±0.08		
	3	Positive slope	L	26.12.2004-08.01.2005	329	27.12.2004 (6.2)	0.64±0.04		
	4	Negative slope	S	08.01.2005-09.12.2012	936	27.11.2007 (6.0), 09.05.2010 (6.6)	0.86±0.03		
	5	Positive slope	L	09.12.2012-06.04.2016	117	-	0.76±0.07		
D	1	Positive slope	L	30.04.1969-26.12.2004	163	-	0.63±0.05	0.7838	0.90±0.03
	2	Horizontal	M	26.12.2004-30.12.2004	190	-	0.94±0.07		
	3	Positive slope	L	30.12.2004-06.01.2005	51	-	0.59±0.08		
	4	Negative slope	S	06.01.2005-09.04.2013	503	24.01.2005 (6.1), 24.07.2005 (6.4), 12.06.2010 (7.0)	1.09±0.05		
	5	Horizontal	M	09.04.2013-22.02.2016	29				
E	1	Positive slope	L	25.04.1965-02.10.1994	445	19.06.1986 (6.0), 15.11.1990 (6.2)	0.60±0.03	0.7952	0.83±0.02
	2	Negative slope	S	02.10.1994 –14.04.2004	297	-	0.95±0.05		
	3	Positive slope	L	14.04.2004 - 26.12.2004	108	26.12.2004 (6.0)	0.66±0.06		
	4	Negative slope	S	26.12.2004-29.01.2005	1004	-	0.95±0.03		
	5	Positive slope	L	29.01.2005-05.02.2005	98	-	0.63±0.06		
	6	Negative slope	S	05.02. 2005-18.02.2013	483	05.09.2011 (6.5)	1.08±0.05		
	7	Positive slope	L	18.02.2013-01.05.2016	333	21.03.2014 (6.4), 08.11.2015 (6.6)	0.73±0.04		
F	1	Positive slope	L	04.04.1966-27.10.1995	125	05.11.1971 (6.0)	0.67±0.06	0.7606	0.97±0.03
	2	Negative slope	S	27.10.1995-04.01.2004	100	-	1.24±0.12		
	3	Positive slope	L	04.01.2004-08.01. 2005	107	-	0.76±0.07		
	4	Negative slope	S	08.01.2005-26.07.2006	196	-	1.24±0.09		
	5	Negative slope	S	26.07.2006-19.08.2012	244	27.06.2008 (6.5)	1.11± 0.07		
	6	Positive slope	L	19.08.2012-09.05.2016	46	-	0.83±0.12		
G	1	Positive slope	L	15.10.1965-03.11.1998	56	24.01.1983 (6.2)	0.54±0.07	0.7702	0.99±0.03
	2	Negative slope	S	03.11.1998-13.10.2002	87	-	1.18±0.13		
	3	Positive slope	L	13.10.2002-27.12.2004	92	26.12.2004 (6.1)	0.70±0.07		
	4	Negative slope	S	27.12.2004-26.07.2008	335	-	1.24±0.07		
	5	Negative slope	S	26.07.2008- 06.05.2013	211	10.08.2009 (6.7), 30.03.2010 (6.5), 18.06.2010 (6.1)	1.09± 0.07		
	6	Positive slope	L	06.05.2013-02.05.2016	56	-	0.75±0.10		

***Table 2.** Contd....*

Zone	Segments (see Figs 3a-i)	Nature of the segment	Nature of clustering (L, M, S)*	Time Period	No. of earthquakes in the segment	Major shock in in the segment (Mw)	b-value of the segment with error	Hurst K coefficient of the zone	b-value of the Zone with error
H	1	Positive slope	L	07.01.1965-09.08.1994	415	14.02.1967 (5.8)	0.62±0.03	0.858	0.81±0.02
	2	Negative slope	S	09.08.1994-01.08.2014	607	31.05.2010 (6.1) 31.07.2014 (6.0)	1.03±0.04		
	3	Positive slope	L	01.08.2014-22.04.2016	45	-	0.73±0.11		
I	1	Positive slope	L	22.01.1965-11.11.1996	145	08.07.1975 (6.0), 29.05.1994 (6.2)	0.65±0.05	0.8552	0.91±0.05
	2	Negative slope	S	11.11.1996- 22.10.2013	169	-	1.41±0.11		
	3	Positive slope	L	22.10.2013-07.03.2016	21	-	0.86±0.19		
J	1	Positive slope	L	26.04.1966-14.04.1995	155	05.01.1991 (6.2) 15.06.1992 (6.0)	0.66±0.05	0.7874	0.84±0.04
	2	Negative slope	S	14.04.1995-18.08.2012	209	-	1.11±0.08		
	3	Positive slope	L	18.08.2012- 22.04.2016	93	11.11.2012 (6.2), 03.04.2013 (6.0), 23.05.2014 (6.0), 30.05.2014 (6.0)	0.76±0.08		
K	1	Positive slope	L	06.05.1966-09.07.1992	52	06.02.1988 (6.0)	0.59±0.08	0.7991	0.91±0.07
	2	Negative slope	S	09.07.1992-19.12.2003	62	11.11.1997 (6.0)	1.21±0.15		
	3	Horizontal	M	19.12.2003-13.12.2009	28	-	0.95±0.18		
	4	Negative slope	S	13.12.2009-21.12.2015	33	-	1.37±0.24		
L	1	Positive slope	L	09.12.1965-24.03.1994	89	17.07.1971 (5.6), 22.09.1984 (5.5), 23.06.1991 (5.6)	0.59±0.07	0.7309	0.93±0.06
	2	Negative slope	S	24.03.1994-30.06.2015	120	-	1.46±0.13		
	3	Horizontal	M	30.06.2015-16.05.2016	12	06.11.2013 (5.6)	0.96±0.16		
M	1	Positive slope	L	30.05.1965-01.09.1991	118	29.07.1970 (6.4), 12.08.1976 (6.2)	0.56±0.06	0.8606	0.85±0.05
	2	Negative slope	S	01.09.1991-27.05.2016	152	07.06.2000 (6.2)	1.21±0.09		
N	1	Positive slope	L	12.01.1965-25.05.1994	116	19.11.1980 (6.0)	0.54±0.06	0.8305	0.82±0.05
	2	Negative slope	S	25.05.94-13.05.1998	45	-	0.97±0.12		
	3	Negative slope	S	13.05.1998-20.07.2009	96	-	1.20±0.12		
	4	Negative slope	S	20.07.2009-19.04.2016	72	21.09.2009 (6.0), 18.09.2011 (6.6)	0.96±0.11		
O	1	Positive slope	L	30.04.1965-24.05.1993	175	-	0.63±0.05	0.8258	0.75±0.04
	2	Negative slope	S	24.05.1993-30.06.2012	113	01.06.2005 (6.0)	1.14±0.11		
	3	Horizontal	M	30.06.2012-11.12.2015	41	-	0.74±0.12		
P	1	Positive slope	L	10.08.1966-16.08.1992	75	-	0.60±0.08	0.7745	1.06±0.06
	2	Negative slope	S	16.08.1992-12.07.1996	65	30.07.1992 (6.0)	1.06±0.11		
	3	Negative slope	S	12.07.1996-26.06.2004	123	-	1.41±0.13		
	4	Negative slope	S	26.06.2004-03.05.2016	74	06.10.2008 (6.1)	1.17±0.14		
Q	1	Positive slope	L	18.02.1965-06.05.1995	429	06.08.1988 (6.6)	0.69±0.03	0.8415	0.91±0.03
	2	Negative slope	S	06.05.1995-11.06.2014	559	04.02.2011 (6.5)	1.30±0.06		
	3	Positive slope	L	11.06.2014-11.06.2016	77	03.01.2016 (6.7), 13.04.2016 (6.9)	0.87±0.07		

*L:Clustering of large magnitude earthquakes/seismic moments; *M:Clustering of moderate magnitude earthquakes/ seismic moments; *S:Clustering of small magnitude earthquakes/seismic moments.

zone E, that in contrast to the other zones from B to G represents an upper plate portion of Burmese-Andaman Arc, shows a prominent decelerating (negative) moment release segments between 05.02.2005 and 18.02.2013 with 483 earthquakes. Zone F evidences a prolonged negative segment between 08.01.2005 and 19.08.2012 of 440 earthquakes, while zone G reflects a prolonged negative segment between 27.12.2004 and 06.05.2013 with 546 earthquakes. Based on the above observations it can be concluded that the lower plate as well as the southern portion of the upper plate of Burmese - Andaman arc system has gone through a prolonged period of elastic strain release

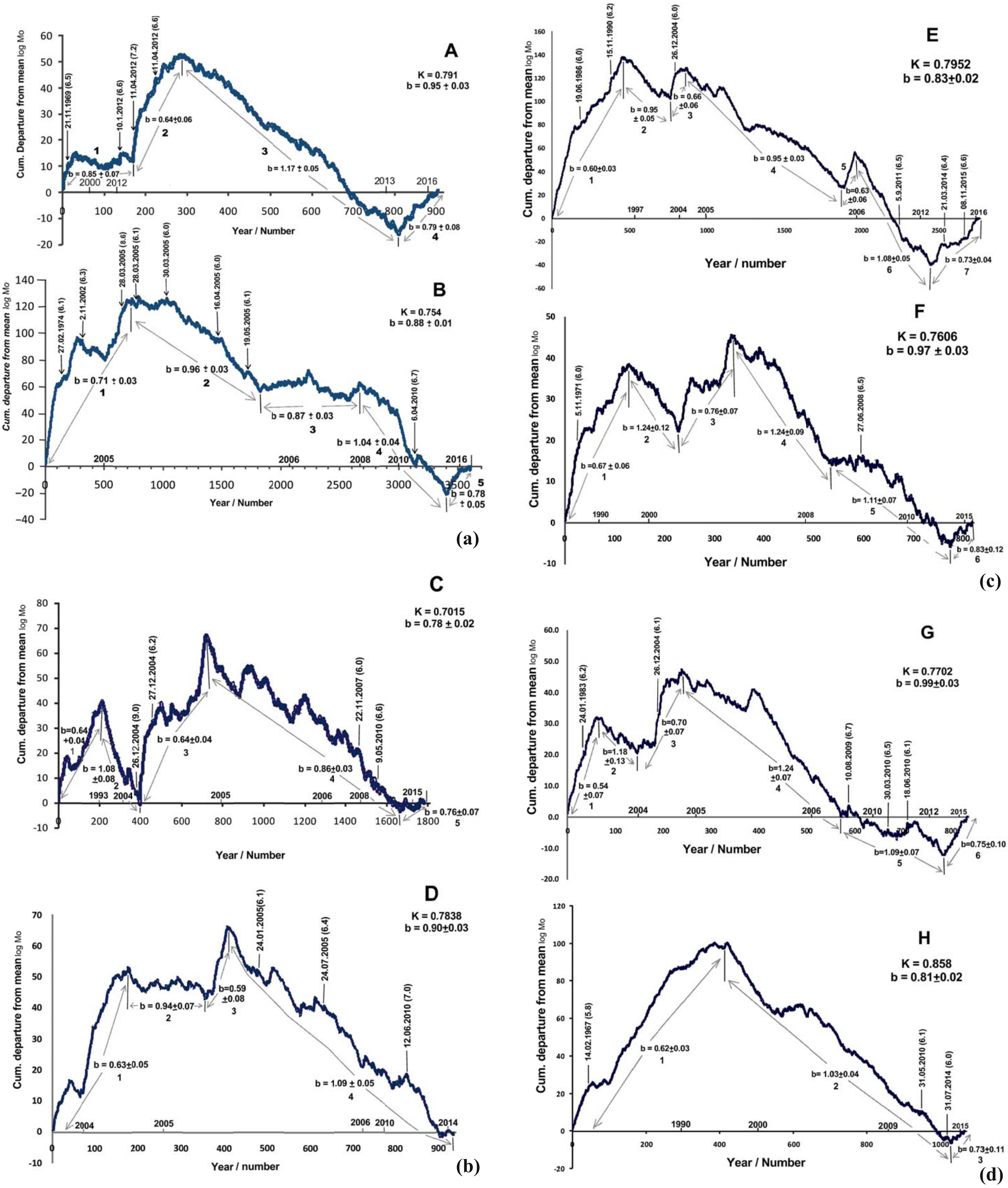

Fig.3. Hurst plot of years against cumulative difference from mean Log cumulative moment release data of earthquakes of seismic zones of Fig.2. Plot indicates temporal clustering and manifested in the plot by alternate horizontal (Clustering of moderate magnitude earthquakes/ seismic moments), positive sloping (Clustering of large magnitude earthquakes/seismic moments) and negative sloping (Clustering of small magnitude earthquakes/seismic moments) moment release segments indicating temporal clustering pattern. (a) Hurst plot of *Zone A* (Indo-Australian Intraplate Zone) in upper panel and *Zone B* (Nias Earthquake Zone) in lower panel), **(b)** Hurst Plot of *Zone C* (Sumatra Earthquake Zone) in upper panel and *Zone D* (NicoberIsland Zone) in lower panel, **(c)** Hurst plot of *Zone E* (Sumatra Island Zone) in upper panel and *Zone F* (South Andaman Zone) in lower panel, **(d)** Hurst plot of *Zone G* (North Andaman Zone) in upper panel and *Zone H* (Andaman Spreading Zone) in lower panel, **(e)** Hurst plot of *Zone I* (South Burma Zone) in upper panel, and *Zone J* (Sagaing Fault Zone) in lower panel, **(f)** Hurst plot of *Zone K* (Tripura Fold Belt and Bangladesh Plain) in upper panel and *Zone L* (Shillong Plateau Zone) in lower panel, **(g)** Hurst plot of *Zone M* (North Burma fold-thrustZone) in upper panel and *Zone N* (NE Himalayan Zone) in lower panel, **(h)** Hurst plot of *Zone O* (Eastern Syntaxis and Jiali Fault Zone) in upper panel and *Zone P* (Tibetan Zone) in lower panel, **(i)** Hurst plot of *Zone Q* (Central Burma Fold Thrust belt).

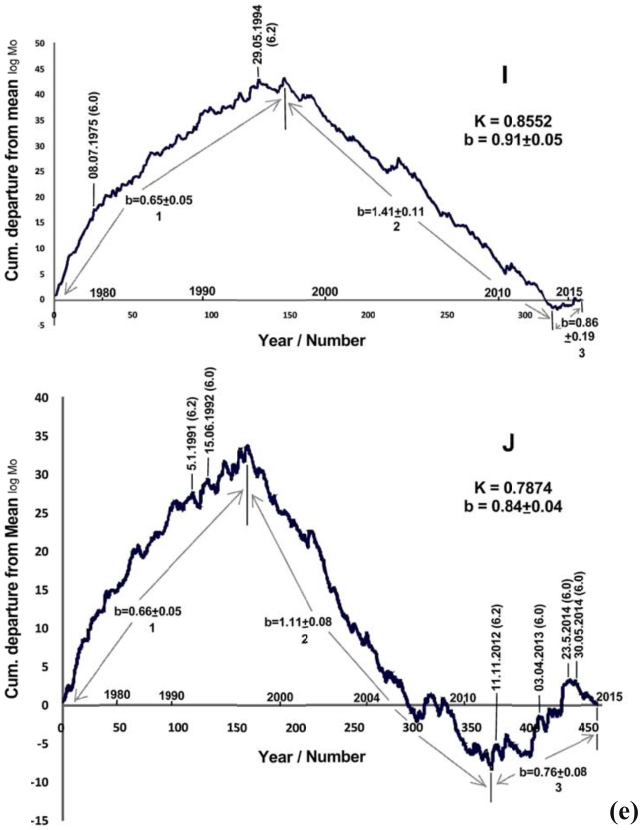

(e)

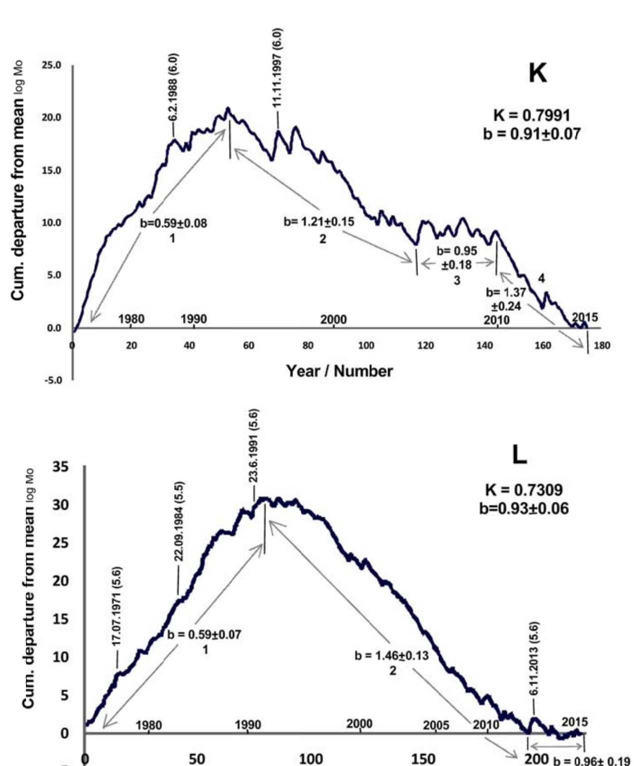

(f)

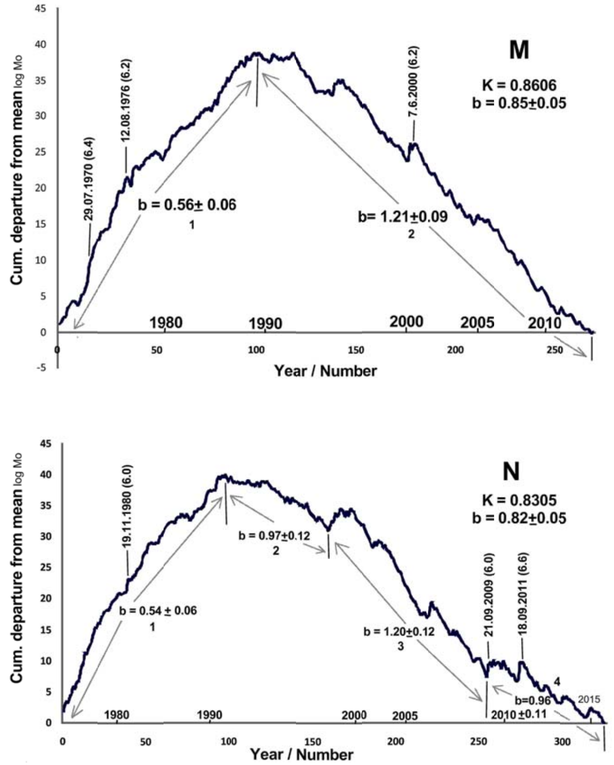

(g)

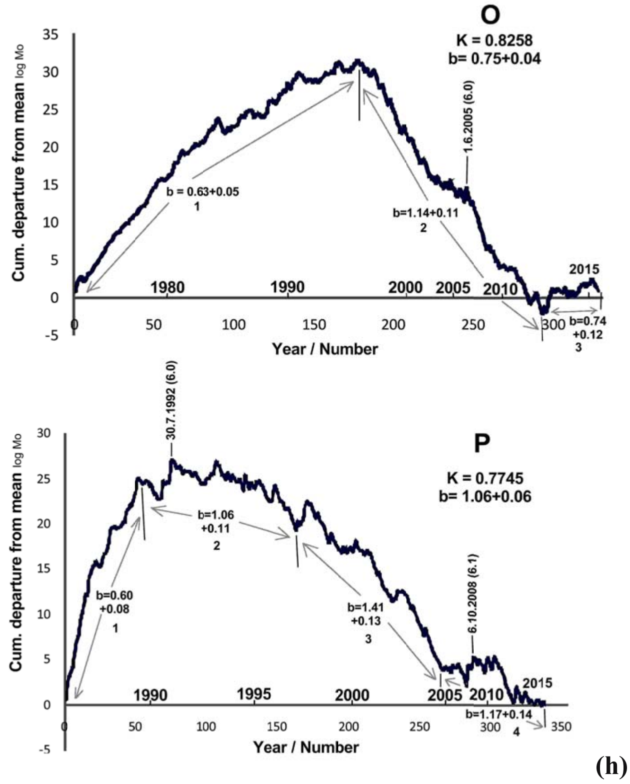

(h)

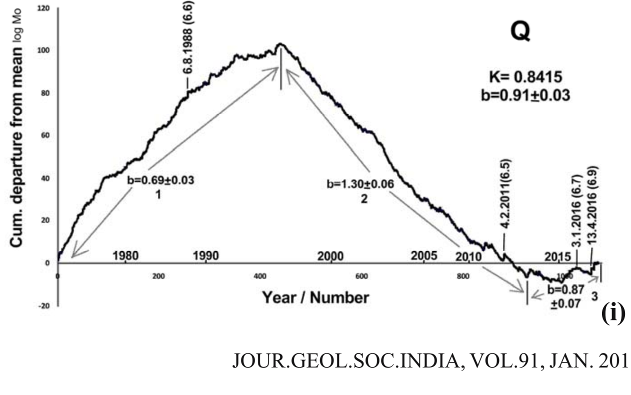

(i)

Fig.3 contd... (e-i) details in previous page.

significantly lower than the average moment release for the year 2005 to 2013. This negative slope eventually ended with a moment release acceleration by positive slope in all the zones of this region to reverse the trend.

In the northern zones, this prominent negative slope in Hurst plots (Figs 3d,e,f,g,i) becomes more extended. The remaining zones of Burmese Andaman arc display a negative slope more prolonged than the rest of the Andaman - Sunda arc. Zone H, representing the upper plate of Burmese Andaman arc, shows a negative segment between 09.08.1994 and 01.08.2014 with 607 earthquakes whereas zone J gives a negative slope from 14.04.1995 to 18.08.2012 with 209 earthquakes. Zone I shows a negative slope between 11.11.1996 and 22.10.2013 with 169 earthquakes; zone K shows two negative segments (between 09.07.1992 and 19.12.2003 with 62 earthquakes and between 13.12.2009 and 21.12.2015 with 33 earthquakes) separated by a notable horizontal segment between 19.12.2003 and 13.12.2009 with 28 earthquakes. Zone L reflects a negative segment between 24.03.1994 and 30.06.2015 with 120 earthquakes while zone Q shows a prolonged negative segment between 06.05.1995 and 11.06.2014 with 559 earthquakes. The negative slope in zone M is even more prolonged. It has continued from 01.09.1991 to 27.05.2016 with 152 earthquakes.

So, from the above mentioned observations it can be concluded that the entire West Sunda arc and the Burmese - Andaman arc give evidence of a prominent period of elastic strain release that starts approximately from year 1995 and continued up to 2015 with three exceptions. (1) The negative sloping segments for zone H and J, both representing the upper plate of BAAS and WSA, end a bit early (2014 for zone H and 2012 for zone J) and a prominent reversal of this negative trend can also be observed (a positive segment between 01.08.2014 and 22.04.2016, with 45 earthquakes for zone H and a positive segment between 18.08.2012 and 22.04.2016 with 93 earthquakes for zone J). (2) Zone K representing the Tripura fold belt and Bangladesh plain displays a notable horizontal segment around year 2005 between two prominent negative segments. (3) The period of negative sloping for zone M starts earlier (around year 1991) than the other blocks.

The period of elastic strain release for NE Himalaya including Tibet (NEHT) is even longer. Zone N gives a negative slope extended from 25.05.1994 to 19.04.2016 (Table 2), zone O gives a negative slope starting from 24.05.1993 to 30.06.2012 (Table 2) and zone P gives negative slope extended from 16.08.1992 to 03.05.2016 (Table 2).

Interestingly, it is observed that the negative sloping segments always end with a high magnitude event to reverse the trend of moment release. So we suggest a prolonged negative segment without a moderate to large earthquake may be regarded as an earthquake precursor. All the zones from B to Q within the study area show evidences of earthquake of magnitude (>6) either at the end phase of the last negative segment or just at the start of horizontal/positive segment immediately after the last negative segment, with only two exceptions for zone I and K. In zone I and zone K, repeatedly representing the south Burma zone and Tripura fold belt and Bangladesh plain, have not yet register any moderate to large earthquake even after an extended period of smaller elastic strain release. So, we conclude this two zones may be treated as seismically vulnerable compared to the others parts of the arc system.

Additionally, it is also clear from the Hurst pattern analysis, that the Hurst plot of one zone often reflects the influences of the most prominent features of the Hurst plot patterns of adjacent zones. So, for zone B to G, though the most prominent negative slope starts approximately at 2005, each zone in this sector also displays another short termed negative slope prior to this as an influence of the northern zones of the region. This early negative/horizontal slope is defined between 28.03.2005 and 30.07.2005 for zone B with 1130 earthquakes, between 13.04.1995 and 26.12.2004 for zone C with 181 earthquakes, between 26.12.2004 and 30.12.2004 for zone D with 190 earthquakes, between 02.10.1994 and 14.04.2004 with 297 earthquakes for zone E, between 27.10.1995 and 04.01.2004 with 100 earthquakes for zone F and between 03.11.1998 and 13.10.2002 with 87 earthquakes for zone G (Table 2).

This character of reflecting features of adjacent Hurst plot patterns explains the above mentioned three exceptions we have observed in the Hurst plot patterns of entire West Sunda arc and Burmese Andaman arc. Early ending of the negative sloping segments for zone H and J is due to the influence of the early ending of the other southern Burmese Andaman arc zones. In the Hurst plots of the zones far north this influence gradually diminishes and we find negative slopes ending late 2015 or even in 2016. Notable horizontal segment of Zone K around year 2005 is also due to its vicinity to the NE – Himalayan zones (Zones O, P, N). In these zones too this horizontal segment or sudden decrease in negative slope can be observed around 2005. Similarly, early instant of negative slope in Zone M is due to its vicinity to the NE Himalayan zones, where the elastic strain release starts a bit early around year 1992.

CONCLUSIONS

Analysing the Hurst plots for each of the seventeen zones and its relationship with the corresponding b-value of each segments within the Hurst pattern, the following conclusions can be drawn.

a) Lack of occurrence of major earthquakes in negative sloping segments indicate decelerated moment release pattern or temporal slackening of elastic strain release compared to the average (mean) moment release rate. This also indicates a temporal clustering of small magnitude earthquakes / seismic moments that exhibit high b–value (> 0.95).
b) The horizontal segment in a Hurst plot indicates temporal clustering of moderate magnitude events / seismic moments with moderate b-values (0.8 – 0.95).
c) The positive segment in a Hurst plot is characterised by accelerated moment release within a short span of time with temporal clustering of larger magnitude earthquakes / seismic moments and exhibit lowest b–value (<0.7).
d) The lower plate as well as the southern portion of the upper plate of Burmese Andaman arc system has gone through a prolonged period of elastic strain release generation earthquakes significantly lower than the average from the year 2005 to 2013.
e) The entire West Sunda arc and the northern portion of the upper plate of the Burmese Andaman arc give evidence of a prominent period of elastic strain release that starts approximately from year 1995 and continued up to 2015.
f) The period of elastic strain release for NE Himalaya including Tibet (NEHT) is even longer and starts approximately from 1992 and continues up to the recent times.
g) The negative sloping segments always end with a high magnitude event to reverse the trend of moment release. So a prolonged negative segment without a moderate to large earthquake may be regarded as an earthquake precursor. Following this, the south Burma zone and Tripura fold belt and Bangladesh plain (zone I and K), have not yet register any moderate to large earthquake even after an extended period of smaller elastic strain release. So this two zones may be treated as seismically vulnerable.

Acknowledgement: Authors thankfully acknowledge with gratitude the interest shown by Dr. B. Mahabaleswar, Editor-in-Chief, to improve the content of the paper. Constructive comments and interest shown by learned reviewer Dr. B.K. Rastogi has considerably improved the quality of presentation and scientific content of the paper.

References

Aki, K. (1965) Maximum likelihood estimate of *b* in the formula log N = a – bM and its confidence limits. Bull. Earthquake Res. Inst., Tokyo Univ., v.43, pp.237-239.

Chen, C., and Hiscott, R.N. (1999) Statistical analysis of turbidite cycles in submarine fan successions: Tests for short term persistence. Jour. Sed. Res., v.69, pp.486-504.

Curray, J.R. (2005) Tectonics and history of the Andaman Sea region. Jour. Asian Earth Sci., v.25, pp.187-232.

Evans, T.E. (1996) The effects of changes in the world hydrological cycle on availability of water resources. *In:* F. Bazzaz and W. Sombrock (Eds.), Global Climate Change and Agricultural Production: Direct and Indirect Effects of Changing Hydrological, Pedological and Plant Physiological Processes, Chapter 2, FAO and John Wiley, Whichester.

Feeder, J. (1988) Fractals, Plenum, New York, 283p.

Feng L., and Zhou, J. (2013) Trend predictions in water resources using rescaled range (R/S) analysis. Environ. Earth Sci., v.68(8), pp.2359–2363.

Hanks, H.C., and Kanamori, H. (1979) A moment magnitude scale. Jour. Geophys. Res. v.84, B5, pp.2348-2350, DOI: 10.1029/JB084iB05p02348.

Haslett, J. and Raftery, A.E. (1989) Space-time modelling with long-memory dependence: assessing Ireland's wind power resource. Appl. Stat., v.38(1) pp.1-50, DOI: 10.2307/2347679.

Hurst, H.E. (1951) Long term storage capacity of reservoirs. Tran. Amer. Soc. Civil Engg., v.16, pp.770-808.

Hurst, H.E. (1956) Methods of using long-term storage in reservoirs. Proc. Inst. Civil Eng., Part 1, 5, pp.519-590.

Hernandez-Martinez, E., Perez-Muñoz, T., Velasco-Hernandez, J. X., Altamira-Areyan, A., Velasquillo-Martinez, L. (2013) Facies Recognition Using Multifractal Hurst Analysis: Applications to Well-Log Data. Mathematical Geosciences, v.45(4), pp.471–486

Koutsoyiannis, D. (2003) Climate change, the Hurst phenomenon, and hydrological statistics. Hydrol. Sci. Jour., v. 48(1), pp.3-24, DOI: 10.1623/hysj.48.1.3.43481.

Mandelbrot, B. and Hudson, R.L. (2004) The (Mis)Behavior of Markets, A Fractal View of Risk, Ruin and Reward. Basic Books – Business & Economics, 328p.

Mansukhani, S. (2012) The Hurst Exponent: Predictability of Time Series. Analytics Magazine**,** IssueJuly/August 2012, http://analytics-magazine.org/the-hurst-exponent-predictability-of-time-series/

Markonis, Y., and Koutsoyiannis, D.(2013) Climatic Variability Over Time Scales Spanning Nine Orders of Magnitude: Connecting Milankovitch Cycles with Hurst–Kolmogorov Dynamics. Surveys in Geophysics, v.34 (2), pp.181–207

McGuire, R.K. (2004) Seismic Hazard and Risk Analysis, EERI Monograph 10, Earthquake Engineering Research Institute, Oakland, California, 221p.

Miao, L., Jiang, C., Xue, B., Liu, Q., He, B., Nath, R., and Cui X. (2015) Vegetation dynamics and factor analysis in arid and semi-arid Inner Mongolia. Environ. Earth Sci., v.73(5), pp.2343–2352.

Mukhopadhyay, B., Chakraborty, P.P., and Paul,S. (2003) Facies clustering in turbidite successions: Case study from Andaman Flysch Group, Andaman Islands, India. Gondwana Res., v.6(4), pp. 918-925, DOI: 10.1016/S1342-937X(05) 71036-4.

Mukhopadhyay, B., Acharyya, A., and Dasgupta, S. (2009) Statistical Analysis on Yearly Seismic Moment Release Data to Demarcate the Source Zone for an Impending Earthquake in the Himalaya. Acta Geophysica, v.57 (2), pp.387-399, DOI: 10.2478/s11600-008-0068-0

Scordilis, E.M. (2006) Empirical global relations converting MS and mb to moment magnitude. Jour. Seismol., v.10, pp.225–236.

Shi, P., Wu, M., Qu, S., Jiang,P., Qiao, X., Chen, X., Zhou, M. and Zhang, Z. (2015) Spatial Distribution and Temporal Trends in Precipitation Concentration Indices for the Southwest China. Water Resources Management, v.29(11), pp.3941–3955.

Wallis, J.R. and Matalas, N.C. (1970) Small sample properties of H and K estimators of Hurst coefficient h. Water Resour. Res., v.6(6), pp.1583-1594, DOI: 10.1029/ WR006i006p01583.

Wallis, J.R., and Matalas, N.C. (1971) Correlogram analysis revisited. Water Resour. Res., v.7(6), pp.1448-1459, DOI: 10.1029/WR007i006p01448.

Wiemer, S. and Wyss, M. (2000) Minimum magnitude of completeness in earthquake catalogs: example from Alaska, the western United States, and Japan. Bull. Seismol. Soc. Amer., v.90(4), pp.859-869.

Weber, R.O. and Talkner, P. (2001) Spectra and correlations of climate data from days to decades. Jour. Geophys. Res., v.106 (D17), pp.20131–20144.

(Received: 25 January 2017; Revised form accepted: 4 May 2017)